

Controlled crossover of electron transport in graphene nanoconstriction: From Coulomb blockade to electron interference

Wei Yu(余炜), Xiao Guo(郭潇), Yuwen Cai(蔡煜文), Xiaotian Yu(俞晓天), and Wenjie Liang(梁文杰)
Citation: Chin. Phys. B, 2023, 32 (**7**): 077202. DOI: 10.1088/1674-1056/accf67
Journal homepage: http://cpb.iphy.ac.cn; http://iopscience.iop.org/cpb

What follows is a list of articles you may be interested in

Tunable correlation in twisted monolayer-trilayer graphene

Dongdong Ding(丁冬冬), Ruirui Niu(牛锐锐), Xiangyan Han(韩香岩), Zhuangzhuang Qu(曲壮壮), Zhiyu Wang(王知雨), Zhuoxian Li(李卓贤), Qianling Liu(刘倩伶), Chunrui Han(韩春蕊), and Jianming Lu(路建明)
Chin. Phys. B, 2023, 32 (**6**): 067204. DOI: 10.1088/1674-1056/acc8c3

Long-range adsorbate interactions mediated by two-dimensional Dirac fermions

Xiaohui Wang(王晓慧), Zhen-Guo Fu(付振国), Zhigang Wang(王志刚), Feng Chi(迟锋), and Ping Zhang(张平)
Chin. Phys. B, 2023, 32 (**5**): 057201. DOI: 10.1088/1674-1056/acae77

Correlated states in alternating twisted bilayer-monolayer-monolayer graphene heterostructure

Ruirui Niu(牛锐锐), Xiangyan Han(韩香岩), Zhuangzhuang Qu(曲壮壮), Zhiyu Wang(王知雨), Zhuoxian Li(李卓贤), Qianling Liu(刘倩伶), Chunrui Han(韩春蕊), and Jianming Lu(路建明)
Chin. Phys. B, 2023, 32 (**1**): 017202. DOI: 10.1088/1674-1056/ac9de4

Electrically tunable spin diode effect in a tunneling junction of quantum dot

Xukai Peng(彭许凯), Zhengzhong Zhang(张正中)
Chin. Phys. B, 2019, 28 (**12**): 127202. DOI: 10.1088/1674-1056/ab53d0

Detection of Majorana fermions in an Aharonov-Bohm interferometer

Shang En-Ming (尚恩明), Pan Yi-Ming (潘义明), Shao Lu-Bing (邵陆兵), Wang Bai-Gen (王伯根)
Chin. Phys. B, 2014, 23 (**5**): 057201. DOI: 10.1088/1674-1056/23/5/057201

Controlled crossover of electron transport in graphene nanoconstriction: From Coulomb blockade to electron interference

Wei Yu(余炜)[1,2], Xiao Guo(郭潇)[1,2], Yuwen Cai(蔡煜文)[1,2], Xiaotian Yu(俞晓天)[1,2], and Wenjie Liang(梁文杰)[1,2,†]

[1] *Beijing National Center for Condensed Matter Physics, Beijing Key Laboratory for Nanomaterials and Nanodevices, Institute of Physics, Chinese Academy of Sciences (CAS), Beijing* 100190, *China*

[2] *School of Physical Sciences, University of Chinese Academy of Sciences, Beijing* 100190, *China*

(Received 16 March 2023; revised manuscript received 12 April 2023; accepted manuscript online 22 April 2023)

The ability to control transport behaviors in nanostructure is crucial for usage as a fundamental research platform as well as a practical device. In this study, we report a gate-controlled crossover of electron transport behaviors using graphene nanoconstrictions as a platform. The observed transport properties span from Coulomb blockade-dominated single electron transmission to electron–wave interference-dominated quantum behavior. Such drastic modulation is achieved by utilizing a single back gate on a graphene nanoconstriction structure, where the size of nanostructure in the constriction and coupling strength of it to the electrodes can be tuned electrically. Our results indicate that electrostatic field by gate voltage upon the confined nanostructure defines both the size of the nanoconstriction as well as its interaction to electrodes. Increasing gate voltage raises Fermi level to cross the energy profile in the nanoconstriction, resulting in decreased energy barriers which affect the size of nanoconstriction and transmissivity of electrons. The gate-tunable nanoconstriction device can therefore become a potential platform to study quantum critical behaviors and enrich electronic and spintronic devices.

Keywords: graphene nanoconstriction, Coulomb blockade, electron interference, gate-tunable

PACS: 72.80.Vp, 73.23.–b, 73.23.Hk, 73.63.–b **DOI:** 10.1088/1674-1056/accf67

1. Introduction

Quantum confinement effect plays an essential role in making novel nanostructures as well as understanding fundamental electronic interactions when are squeezed together. The sizes of the nanostructures and potential barriers between them and surrounding electrodes play a key role, as have been studied in both theoretical and experimental works, such as two-dimensional (2D) electron gas[1] and nanomaterials,[2,3] one-dimensional (1D) nanotubes,[4–6] and nanoribbons,[7] and zero-dimensional (0D) quantum dots,[8,9] and single molecule transistors.[10,11] Transmission of charge carriers is also of great significance, influencing particle-in-a-box state, p–n junctions, quantum dots states, and Fabry–Perot interference in carbon nanotubes waveguides,[12] revealing different functionalities.[13–16] The ability to reversibly *in-situ* tuning sizes and/or potential barriers would enable different quantum state transitions and in turn change functionalities in a single device without complicated fabrications. Yet, easy control of functionality in nanostructures is still a dawning task.[17,18]

Graphene,[19,20] due to its 2D properties, rose to be an idea material for controllable nanodevices and a platform for fundamental research. Sizes tuning and potential barriers modulation have been carried out on the platform of graphene nanoconstrictions,[21] using techniques such as mechanical stress,[22] and feedback-controlled electromigration,[23] in which transitions of transport behaviors have been observed. The latter can prepare extremely narrow nanostructures of several nanometers with a rather simple fabrication process than the typical plasma etching method. Another approach utilizes electrical field modulation to raise the Fermi level, crossing complicate disorder potential profile,[18] forming different graphene islands or delocalizing charge carriers along the edges of nanoconstrictions.[24] However, wide reversible modulation of transport behaviors and transitions between different transport regimes has yet to be realized in a single nanostructure device.

In this work, a reversibly controllable nanoconstriction device has been achieved where electron transport behaviors stretch across three different regimes tuned controlled by a single back gate. Electron transverses through our nanoconstriction devices behaving changes from quantum particles to quantum wave at different gate voltage settings. Deducing the size of the nanoconstriction in these regions as well as studying characteristics of transport patterns, we conclude that back-gate modulation rises up Fermi level leading to a reduction of barriers between the nanoconstriction and electrodes, transmissivity of electrons, and effective size of the nanoconstriction.

2. Experimental details

2.1. Device fabrication

To make a nanoconstriction device of nanometer scale, we utilize a controlled electromigration technique. First, a graphene flake on the order of tens of micrometers is mechanically exfoliated[25] onto a 300-nm SiO_2/Si substrate that has

†Corresponding author. E-mail: wjliang@iphy.ac.cn

© 2023 Chinese Physical Society and IOP Publishing Ltd

been subjected to O_2 plasma cleaning beforehand. Then, few-layer graphene flake is transferred to a hexagonal boron nitride (h-BN) flake with thickness of 10 nm–40 nm using dry-transfer technique[26] to reduce contaminants in between. h-BN has an atomically smooth surface and is free of dangling bonds and charge traps so that it is a perfect dielectric material for graphene.[27] The other surface of graphene remains to be exposed to atmosphere for oxidation reaction in the following breaking process. That helps to prevent formations of branches of benzene and/or carbon chains.[28,29] Graphene and h-BN then are annealed in an Ar/H_2 mixture flow at 350 °C for 2 hours to further get rid of contaminations from tapes and organic adhesives before and after transfer.

Standard electron beam lithography (EBL) and thermal evaporation of 80-nm Au/4-nm Cr metal are performed to make a graphene channel with length about 1 μm (Fig. 1(a)). Another EBL and O_2 plasma etching are carried out to get ∼ 1.7-μm wide graphene ribbons. Before breaking process, the graphene stripe shows a linear current–bias (I_{sd}–V_{sd}) response curve with a two-terminal resistance around 2.9 kΩ and is p-doped with a charge neutrality point (CNP) around back voltage $V_{bg} = 30$ V (Fig. 1(c)).

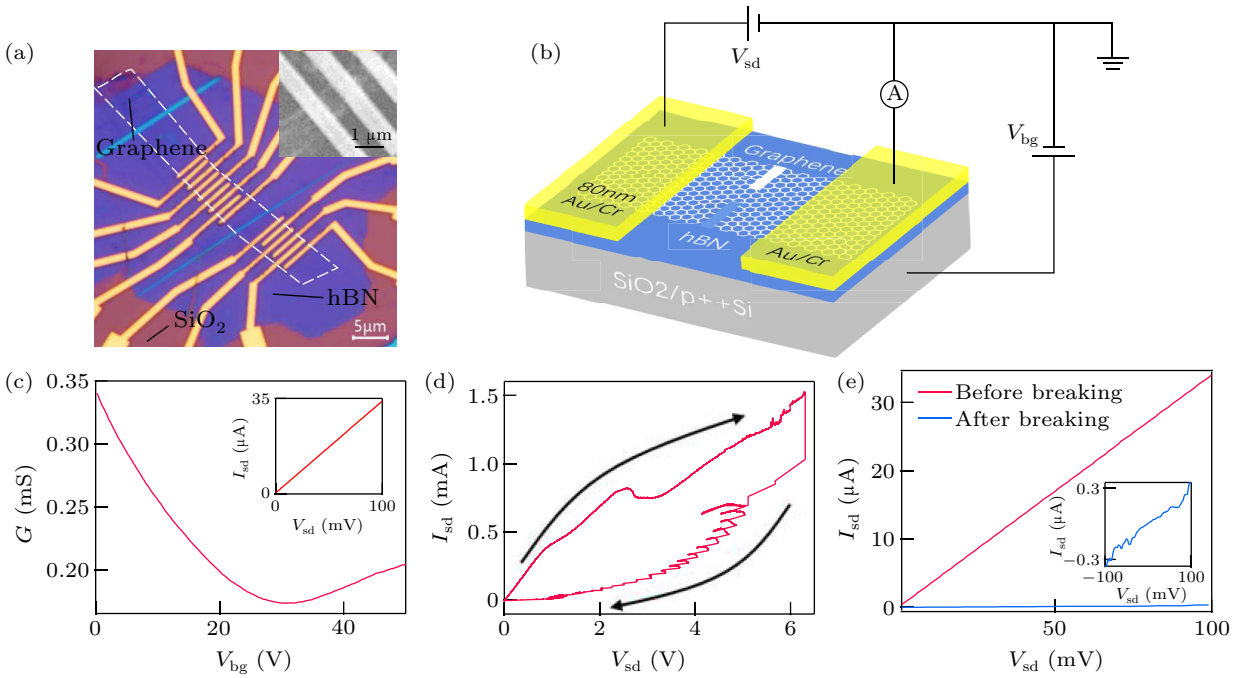


Fig. 1. Schematic diagrams of a device and the feedback-controlled electromigration. (a) An optical image of an hBN-graphene stacked heterojunction device with the SiO_2/Si substrate appearing in rufous, h-BN in blue, the Au/Cr electrodes in yellow, and graphene before etching in white dashed frame. The inset is a scanning electron microscope (SEM) image of this device. (b) A schematic diagram of a graphene nanoconstriction and the measurement circuit. (c) Conductance as a function of back gate voltage V_{bg} recorded at $V_{sd} = 100$ mV before breaking. The inset is a current–bias (I_{sd}–V_{sd}) linear response curve. (d) I_{sd}–V_{sd} traces recorded during feedback-controlled electromigration process. The bias voltage sweeping routine is shown as black curves with arrows. (e) Current traces as a function of V_{sd} before and after breaking shown in red and blue.

Then feedback-controlled electromigration process is performed to achieve nanoconstrictions determined by the setting resistance threshold, at room temperature in air. We ramp up the direct current (dc) voltage between source and drain electrodes while monitoring the current with a 5-kHz sampling rate. At a critical current density, the graphene structure would break and fail, resulting in a resistance increase. Applied voltage will automatically decrease when sample resistance increases by 10% and ramps up again until the target resistance threshold 0.3 MΩ is reached (Fig. 1(d)). After breaking, the I_{sd}–V_{sd} curve deviates from Ohmic response (Fig. 1(e)). The resistance threshold is two orders of magnitude larger than before breaking, but several orders smaller than that in completely breaking graphene nanogaps,[30,31] which preliminarily indicates formation of a nanoconstriction.

2.2. Electronic measurements

Transport investigations are performed in our helium-III refrigerator (Oxford instrument) with a base temperature of 260 mK. Differential conductance (dI/dV) against bias and gate voltages (V_{sd} & V_{bg}) of as made nanoconstriction is measured by standard lock-in technique (Stanford Research SR830) through a data acquisition board (National Instruments, PCI 6289) together with a LabVIEW program. A low-noise current amplifier (DL instrument 1211) is used to convert current to voltage.

3. Results and discussion

A gate voltage which applies a vertical electrical field to our nanoconstriction structure is swept from −60 V to 45 V

while DC bias voltage between source and drain electrodes is kept at zero volt. As gate voltage V_{bg} increases from −60 V to 40 V, dI/dV exhibits remarkable changes by 20 times, 0.02 e^2/h (e, the electron charge; h, Planck's constant) at $V_{bg} = -60$ V to 0.43 e^2/h at 40 V (Fig. 2(a)). A clear distinction of gate depends is observed. dI/dV has a very small value (around 20 nS) and remains unchanged when gate voltage V_{bg} is $-60\ \text{V} < V_{bg} < -20$ V. dI/dV has a higher average value (1.6 μS) and forms series of peaks oscillations separated by regime with negligible conductance when $-16\ \text{V} < V_{bg} < 25$ V. dI/dV increases significantly when $26\ \text{V} < V_{bg} < 45$ V, with an averaged value of 13 μS and non-zero quasi-periodic oscillations. These features could be measured reversibly.

To understand these distinct electron transport behaviors in a single device, we measure dI/dV as a function of gate and bias voltages, V_{bg} and V_{sd} (Fig. 2(b)). Three types of transport behaviors are reproduced (marked by dashed rectangles) in these measurements and a crossover in three transport patterns is found. dI/dV shows negligible value of conductance with weak fluctuation in the regime $-60\ \text{V} < V_{bg} < -35$ V, a sequence of diamonds of varying size in the region $-30\ \text{V} < V_{bg} < 10$ V and checkerboard-like pattern in the region $20\ \text{V} < V_{bg} < 40$ V, respectively. Saturation of false color in map ($35\ \text{V} < V_{bg} < 40$ V) is just a result of color processing for making higher contrast for rest of map.

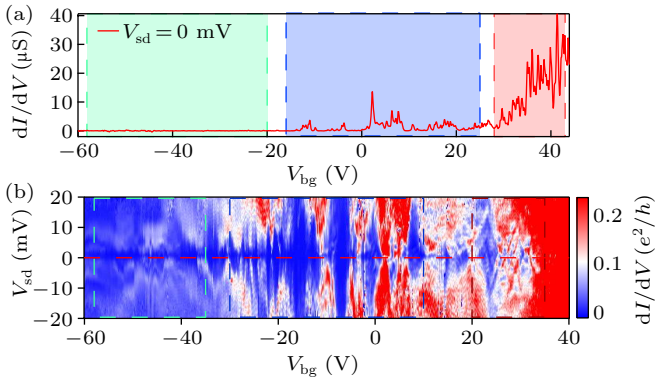


Fig. 2. Electron transport spectra of a graphene nanoconstriction. (a) Trace of V_{bg} dependence of differential conductance (dI/dV) at $V_{sd} = 0$ mV, in which three regions are shown as light green, light blue, and rosered rectangles. (b) False color image of dI/dV as a function of V_{sd} and V_{bg}. Three different transport regions, tunneling-like region, Coulomb blockade region, and electron interference region are shown by dashed boxes corresponding to those in panel (a), respectively. The horizontal red dashed line is corresponding to trace in panel (a).

3.1. Tunneling-like transport

In the first region, the transport behavior is characterized by a tunneling-like nonlinear I_{sd}–V_{sd} response curve but with much larger current than that in a typical graphene nanogap[30] (Fig. 3(b)). Besides, figure 3(a) shows dI/dV plots as a function of V_{bg} and V_{sd}, exhibiting negligible back gate response similar to that in previous nanogaps work,[23] despite some random non-producible high conduction sections with a typical value of 0.5 μS which may be attributed to instability of our graphene nanoconstriction.[29] The low conductance and lack of gate control in this region indicate the nanoconstriction forms a non-transmissive region to electrons. A directly tunneling process occurs in a finite high and nanometer wide barrier in the nanoconstriction, as shown in Fig. 3(e).

3.2. Coulomb blockade

In the second region, a more detailed measurement is performed in V_{bg} ($-28\ \text{V} < V_{bg} < -12$ V) and V_{sd} (±10 mV) region (Fig. 3(c)). A long sequence of diamonds-like dI/dV can be seen. The spike-like dI/dV and its linear dependence to V_{bg} and V_{sd}, the negligible conductance in between the dI/dV lines are in total agreement with the single electron resonant tunneling mechanism. One and only one electron can pass through this nanoconstriction at any specific time when its energy matches the energy level inside the structure and Coulomb repulsion between electrons is compensated by the gate voltage. In other seniors, the transport process is blocked by the Coulomb repulsion between electrons occupying the nanostructure. This is called Coulomb blockade. In our devices, geometry parameters of each diamond have slight changes, of which the slopes are almost unchanged and width (ΔV_{bg}) and height (ΔV_{sd}) vary on small scales of 0.5 V–2.4 V and 4 mV–20 mV, comparable to those in similar systems.[21,22,32,33] Besides, the values of dI/dV are strongly suppressed and are quite different inside and outside the diamonds, ranging from 0 e^2/h to 0.07 e^2/h and from 0.1 e^2/h to 0.2 e^2/h ($\ll 1$ e^2/h) respectively. The V_{bg} dependence of dI/dV for zero bias shows a series of peaks located at the vertexes of diamonds and separated by fragments of zero value (Fig. 3(d)). And change in V_{bg} and V_{sd} can lead the energy level totally in and out the potential window, leading to conductive and blocked states, respectively.

Information about the nanoconstriction can be directly achieved by using Coulomb blockade theory. The charge addition energy E_{add} which is an important quantity to estimate the sizes of quantum dots, is obtained from the height of each diamond ΔV_{sd} (4 meV to 20 meV). $E_{add} = e^2/C_{total} + \Delta E \approx e^2/C_{total} = \alpha e^2/C_G$, when energy spacing ΔE is negligible, where C_G (C_{total}) is capacity between nanoconstriction and gate (surroundings) and $\alpha = C_G/C_{total}$ is called the lever arm equaling to the ratio of $\Delta V_{sd}/\Delta V_{bg}$. We obtain a rough estimate for the size of the graphene nanoconstriction by modeling nanoconstriction area as a circular plate capacitor with $d = \sqrt{4C_G t/\varepsilon_0 \varepsilon_{bg} \pi}$, ε_0 is the vacuum permittivity, t and ε_{bg} are the thickness and the relative dielectric constant of the back gate dielectric layer, respectively. Finally, we have $t/\varepsilon_{bg} \sim 81.92$ nm and extract $\alpha \sim 6.7 \times 10^{-3}$, yielding $d \sim 28$ nm–59 nm, comparable to those in other works.[18,22]

Above analysis indicates that in the second region, this

nanoconstriction behaves like an electron island entrapped by two tunneling barriers to graphene leads in which the extension area of electrons is formed other than the scenario in the first region (Fig. 3(e)).

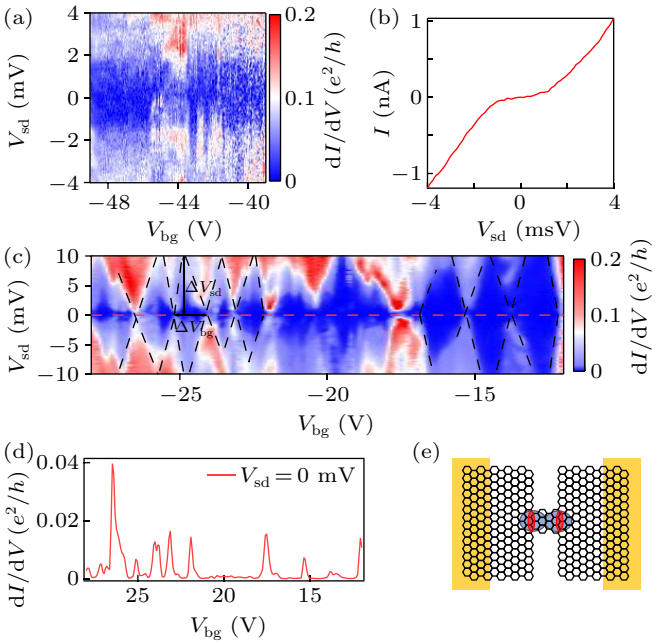


Fig. 3. Directly tunneling through a barrier and Coulomb blockade regions. (a) Plots of dI/dV as a function of V_{sd} and V_{bg} from −49 V to −39 V. (b) I_{sd}–V_{sd} response curve in panel (a). (c) Plots of dI/dV as a function of V_{sd} and V_{bg} from −28 V to −12 V. Several blue diamonds are denoted as crossing dashed lines. Addition energy $E_{add} = \Delta V_{sd}$ and level arm $\alpha = \Delta V_{sd}/\Delta V_{bg}$ are extracted from diamonds marked by arrows. The horizontal red dashed line corresponds to trace in panel (d). (d) Trace of V_{bg} dependence of dI/dV at $V_{sd} = 0$ mV. (e) Schematic diagram of changes in barriers of the two transport regions. Blue and red ovals represent barriers in lower and higher gate ranges, respectively. And scope of delocalized electrons in the nanoconstriction gets larger as V_{bg} increases, shown as the portion between two barriers of the same color.

3.3. Electron interference

Figure 4(a) shows electron transport behavior in the third and most conductive region, exhibiting a checkerboard pattern in the dI/dV false color map as a function of gate (27 V $< V_{bg} <$ 37 V) and bias (±4 meV) voltages. dI/dV increases from 0.05 e^2/h to 0.47 e^2/h. Further, it keeps increasing up to a value, 0.9 e^2/h at higher V_{bg}, shown in Fig. 4(d). The checkerboard pattern is marked by quasi-periodic crossing peaks (valleys) lines with vertical distances (twice the energy spacing, $2E$) in V_{sd} ranging from 1.5 meV to 2.5 meV. dI/dV in all valleys is far from zero, indicating electron transport process is not blocked as in the Coulomb blockade mechanism. As shown in Fig. 4(b), zero bias dI/dV trace against gate voltage (30 V $< V_{bg} <$ 33 V) shows sine oscillations with two different periods (around 0.156 V, 0.248 V), amplitudes (around 0.02 e^2/h, 0.03 e^2/h) and averages (around 0.05 e^2/h, 0.10 e^2/h). Figure 4(c) shows a fast Fourier transform (FFT) of Fig. 4(a), having four branches of highlighted peak clusters on the diagonal implying quasi periodicity of the dI/dV oscillations, with small contrast. The energy spacing can be simply extracted from the dashed ovals,[34] which ranges from 0.74 meV to 1.2 meV. In addition, from the temperature dependence of oscillations in a higher gate (50 V $< V_{bg} <$ 63 V) range measurements shown in Fig. 4(d), the periods and amplitudes of oscillations remain unchanged until temperature reaches 10 K–12 K, corresponding to thermal electron thermal motion energy of 0.86 meV–1.03 meV, comparable to energy spacing E above. The non-zero oscillations with none temperature dependence indicates that this quasi-periodic transport pattern could be attributed to a multi-mode Fabry–Perot interference.[23,34] Electron forms a constructive or destructive interference when going through our nanoconstriction devices, depending on its wave length changes upon gate modulation. The transmission or the conductivity of our tiny nanodevice are total determined by electrons' wave nature.

In this region, electron mean free path is comparable to or larger than sample sizes. Further, the ratio of width W and length L of samples determines whether it is periodic single-mode or quasi-periodic multi-mode Fabry–Perot interference. In case of $L \ll W$ or $W \to 0$, longitudinal modes always dominate in transport and conductance maps and fast Fourier transforms (FFTs) of them are generally with high contrast. While L and W turn to be comparable, longitudinal and transverse modes coexist and it exhibits quasi-periodic multimode patterns in conductance maps, resulting in smaller contrast in FFTs. Using a-particle-in-a-box approximation, we have relevant length scale formula $l = h v_F/(2E)$, where v_F is the Fermi velocity for graphene. Using $v_F = 1 \times 10^6$ m/s, we estimate l is about 1.8 μm–2.8 μm, slightly larger than the sizes of our graphene channels. This indicates that, in this region, height and width of barriers between graphene leads and nanoconstriction decrease to result in an increase in transmissivity so that electrons propagate in the whole channel through the nanoconstriction and then reflect off the metal–graphene contact to form interference with an enhancement of dI/dV in oscillations against V_{bg}, as shown in Fig. 4(e).

However, we cannot exclude the existence of other type of interference, such as universal conductance fluctuations (UCF). Electrons are predominantly scattered by impurities but keep coherent after several different scattering paths, resulting in interference patterns. In graphene samples, UCF oscillations are prominent near Dirac point and have a modulation on Fabry–Perot interference patterns which turns into intermediate peaks in FFTs.[34] In our case, the gate section from 27 V to 37 V, is exactly near the Dirac point of this device, with lower carrier velocity and unknown complicated edge disorders after electromigration process which may intensively scatter electrons. Therefore, UCFs may partially account for this interference pattern.[34–36]

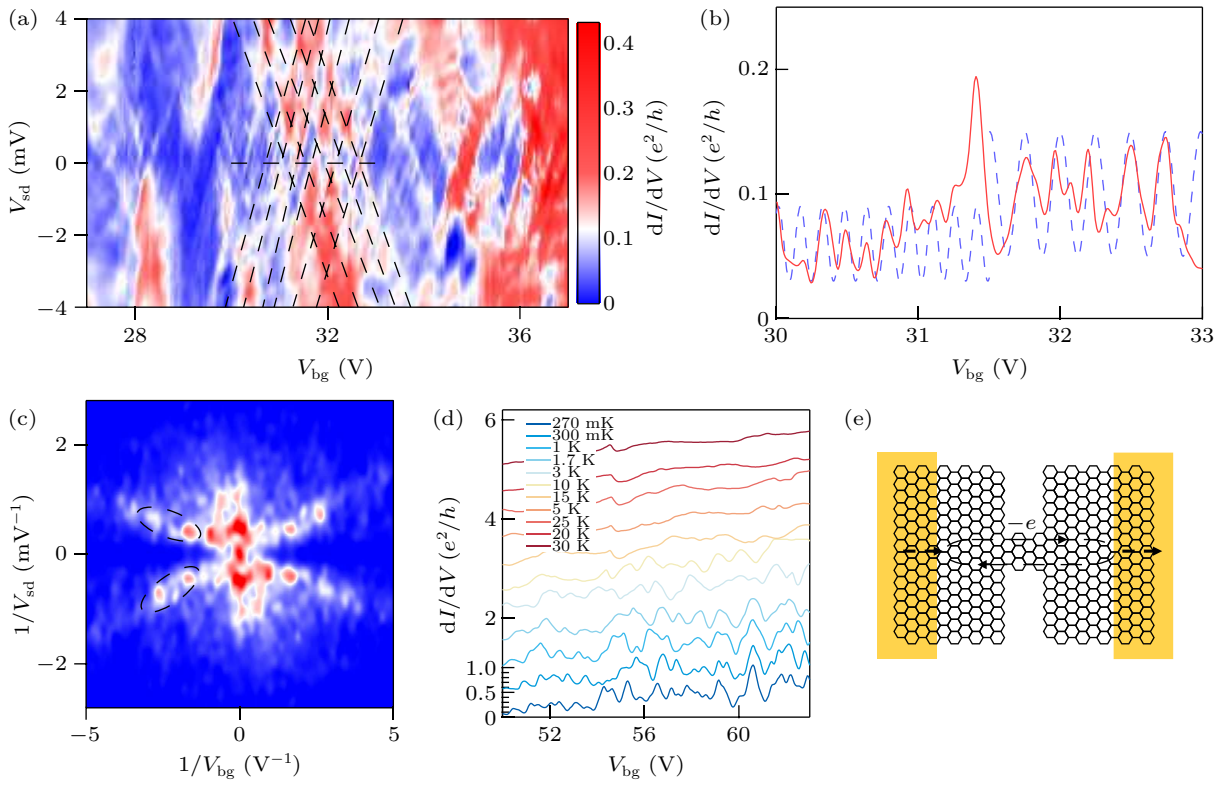


Fig. 4. Electron interference in a higher back voltage region. (a) Plots of dI/dV as a function of V_{sd} and V_{bg} from 27 V to 37 V. It exhibits a checkerboard-like interference pattern, partially displayed as a dashed grid. The horizontal dashed line is corresponding to the trace in panel (b). (b) Trace of dI/dV against V_{bg} at zero bias. Two dashed sine curves are used to fit the trace to estimate the periodicity of oscillations. (c) Fast Fourier transform (FFT) of plots in panel (a). It has been slightly smoothed for clarity. Two dashed ovals encircle two of four diagonal petals of peak clusters, from which we can deduce the energy spacing. (d) Temperature dependence of interference. The increase in T is indicated by the color variation from blue to red. These curves are vertically offset by 0.6 e^2/h for clarity. As temperature reaches 10 K, oscillations start disappearing. (e) Schematic diagram of electron interference. Black dashed curves represent the paths of one electron in the junction. Electrons reflect at the boundary of the metal–graphene contacts due to the potential barriers between them.

4. Conclusion and perspectives

Successful realization of three types of transport behavior and device functions in one graphene nanostructure has been achieved in this study. It opens up a new possibility of using graphene nanostructure as novel devices or a platform for quantum transport of elections. The electrical control of these behaviors is handy compared to mechanical stretching or etching devices into different shapes. Above observation infers that the practical size of the nanoconstriction that is responsible for electron transport changes with electrostatic field applied by the gate. Numerical calculations[37–39] have shown that external electrical field can change transmission probabilities in graphene nanoconstriction, consisting with other experimental works.[17,18] Our gate-controlled modulation thus can be tribute to the following mechanism. Increase of gate voltage results in Fermi level rising in the nanoconstriction, leading to a decrease of height and width of energy barriers between the nanoconstriction and graphene leads. This changing of energy profile in nanoconstriction device in turn results in an enlargement of valid area in nanoconstriction to couple to electrode and an increase of transmissivity of electrons through barriers. Thus, dominating factors governing the electron transport change in three regimes in different gate regions, shown as a crossover in conductance maps.

In summary, a crossover in transport regimes spanning from directly tunneling through a barrier with almost localized electrons in nanoconstriction, to Coulomb blockade of graphene quantum dots of $\sim 10^1$ nm, then to electron interference through nanoconstriction in the whole graphene channel of ~ 1 μm, is observed in our nanoconstriction device tuned by a single back gate. The transport mechanism changes from particle picture to electron wave picture in single device due to gate dependent energy profile inside the constriction area. Such a system can play as the simplest, crucial, and fundamental building blocks in future electric devices. Although a well-defined quantum dot is not formed in nanoconstrictions prepared by electromigration due to the random local configuration with edge defects and tunable barriers, we can improve this by preparing graphene being encapsulated by two hBN flakes and etched into small constrictions by plasma, then being electro-burned in pure oxygen atmosphere, and undergoing longtime current cycles for stableness finally. Furthermore, benefiting from two large areas of graphene leads which can be tuned in a well-designed gate structure separately from nanoconstriction, we anticipate this platform will have further benefits in developing novel electronics and spintronics.

Acknowledgments

Project supported by the National Basic Research Program of China (Grant No. 2016YFA0200800), the Strategic Priority Research Program of the Chinese Academy of Sciences (Grant Nos. XDB30000000 and XDB07030100), and the Sinopec Innovation Scheme (Grant No. A-527).

References

[1] Klitzing K V, Dorda G and Pepper M 1980 *Phys. Rev. Lett.* **45** 494
[2] Novoselov K S, Geim A K, Morozov S V, Jiang D, Zhang Y, Dubonos S V, Grigorieva I V and Firsov A A 2004 *Science* **306** 666
[3] Mak K F, Lee C, Hone J, Shan J and Heinz T F 2010 *Phys. Rev. Lett.* **105** 136805
[4] Tans S J, Verschueren A R M and Dekker C 1998 *Nature* **393** 49
[5] White C T and Todorov T N 1998 *Nature* **393** 240
[6] Fang J H, Liu L W, Kong W J, Cai J Z and Lü L 2006 *Chin. Phys. B* **15** 1071
[7] Han M Y, Özyilmaz B, Zhang Y and Kim P 2007 *Phys. Rev. Lett.* **98** 206805
[8] Goldhaber-Gordon D, Göres J, Kastner M A, Shtrikman H, Mahalu D and Meirav U 1998 *Phys. Rev. Lett.* **81** 5225
[9] Sasaki S, De Franceschi S, Elzerman J M, van der Wiel W G, Eto M, Tarucha S and Kouwenhoven L P 2000 *Nature* **405** 764
[10] Liang W J, Shores M P, Bockrath M, Long J R and Park H 2002 *Nature* **417** 725
[11] Park J, Pasupathy A N, Goldsmith J I, Chang C, Yaish Y, Petta J R, Rinkoski M, Sethna J P, Abruña H D, McEuen P L and Ralph D C 2002 *Nature* **417** 722
[12] Liang W, Bockrath M, Bozovic D, Hafner J H, Tinkham M and Park H 2001 *Nature* **411** 665
[13] Loss D and DiVincenzo D P 1998 *Phys. Rev. A* **57** 120
[14] Appenzeller J, Lin Y M, Knoch J and Avouris P 2004 *Phys. Rev. Lett.* **93** 196805
[15] Wang L J, Cao G, Tu T, Li H O, Zhou C, Hao X J, Su Z, Guo G C, Jiang H W and Guo G P 2010 *Appl. Phys. Lett.* **97** 262113
[16] Ionescu A M and Riel H 2011 *Nature* **479** 329
[17] Stampfer C, Schurtenberger E, Molitor F, Güttinger J, Ihn T and Ensslin K 2008 *Nano Lett.* **8** 2378
[18] Stampfer C, Güttinger J, Hellmüller S, Molitor F, Ensslin K and Ihn T 2009 *Phys. Rev. Lett.* **102** 056403
[19] Novoselov K S, Geim A K, Morozov S V, Jiang D, Katsnelson M I, Grigorieva I V, Dubonos S V and Firsov A A 2005 *Nature* **438** 197
[20] Zhang Y, Tan Y W, Stormer H L and Kim P 2005 *Nature* **438** 201
[21] Moser J and Bachtold A 2009 *Appl. Phys. Lett.* **95** 173506
[22] Caneva S, Hermans M, Lee M, García-Fuente A, Watanabe K, Taniguchi T, Dekker C, Ferrer J, van der Zant H S J and Gehring P 2020 *Nano Lett.* **20** 4924
[23] Gehring P, Sadeghi H, Sangtarash S, Lau C S, Liu J J, Ardavan A, Warner J H, Lambert C J, Briggs G A D and Mol J A 2016 *Nano Lett.* **16** 4210
[24] Bischoff D, Libisch F, Burgdörfer J, Ihn T and Ensslin K 2014 *Phys. Rev. B* **90** 115405
[25] Huang Y, Sutter E, Shi N N, Zheng J, Yang T, Englund D, Gao H J and Sutter P 2015 *ACS Nano* **9** 10612
[26] Kim K, Yankowitz M, Fallahazad B, Kang S, Movva H C P, Huang S, Larentis S, Corbet C M, Taniguchi T, Watanabe K, Banerjee S K, LeRoy B J and Tutuc E 2016 *Nano Lett.* **16** 1989
[27] Dean C R, Young A F, Meric I, Lee C, Wang L, Sorgenfrei S, Watanabe K, Taniguchi T, Kim P, Shepard K L and Hone J 2010 *Nat. Nanotechnol.* **5** 722
[28] Standley B, Bao W, Zhang H, Bruck J, Lau C N and Bockrath M 2008 *Nano Lett.* **8** 3345
[29] Sadeghi H, Mol J A, Lau C S, Briggs G A D, Warner J and Lambert C J 2015 *Proc. Natl. Acad. Sci. USA* **112** 2658
[30] Ullmann K, Coto P B, Leitherer S, Molina-Ontoria A, Martin N, Thoss M and Weber H B 2015 *Nano Lett* **15** 3512
[31] Sun H T, Jiang Z L, Xin N, Guo X F, Hou S M and Liao J H 2018 *ChemPhysChem* **19** 2258
[32] Leturcq R, Stampfer C, Inderbitzin K, Durrer L, Hierold C, Mariani E, Schultz M G, von Oppen F and Ensslin K 2009 *Nat. Phys.* **5** 327
[33] Wang L J, Cao G, Tu T, Li H O, Zhou C, Hao X J, Guo G C, Guo G P 2011 *Chin. Phys. Lett.* **28** 067301
[34] Oksanen M, Uppstu A, Laitinen A, Cox D J, Craciun M F, Russo S, Harju A and Hakonen P 2014 *Phys. Rev. B* **89** 121414
[35] Horsell D W, Savchenko A K, Tikhonenko F V, Kechedzhi K, Lerner I V and Fal'ko V I 2009 *Solid State Commun.* **149** 1041
[36] Berezovsky J, Borunda M F, Heller E J and Westervelt R M 2010 *Nanotechnology* **21** 274013
[37] Muñoz-Rojas F, Jacob D, Fernández-Rossier J and Palacios J J 2006 *Phys. Rev. B* **74** 195417
[38] Huang L, Lai Y C, Ferry D K, Akis R and Goodnick S M 2009 *J. Phys.: Condens. Matter* **21** 344203
[39] Motta C, Sánchez-Portal D and Trioni M I 2012 *PCCP* **14** 10683